Cross Talk among Calcium, Hydrogen Peroxide, and Nitric Oxide and Activation of Gene Expression Involving Calmodulins and Calcium-Dependent Protein Kinases in *Ulva compressa* Exposed to Copper Excess[1][C][W][OA]

Alberto González, M. de los Ángeles Cabrera, M. Josefa Henríquez, Rodrigo A. Contreras, Bernardo Morales, and Alejandra Moenne*

Departamento de Biología, Facultad de Química y Biología, Universidad de Santiago de Chile, 9170022 Santiago, Chile

To analyze the copper-induced cross talk among calcium, nitric oxide (NO), and hydrogen peroxide (H_2O_2) and the calcium-dependent activation of gene expression, the marine alga *Ulva compressa* was treated with the inhibitors of calcium channels, ned-19, ryanodine, and xestospongin C, of chloroplasts and mitochondrial electron transport chains, 3-(3,4-dichlorophenyl)-1,1-dimethylurea and antimycin A, of pyruvate dehydrogenase, moniliformin, of calmodulins, *N*-(6-aminohexyl)-5-chloro-1-naphtalene sulfonamide, and of calcium-dependent protein kinases, staurosporine, as well as with the scavengers of NO, 2-(4-carboxyphenyl)-4,4,5,5-tetramethylimidazoline-1-oxyl-3-oxide, and of H_2O_2, ascorbate, and exposed to a sublethal concentration of copper (10 μM) for 24 h. The level of NO increased at 2 and 12 h. The first peak was inhibited by ned-19 and 3-(2,3-dichlorophenyl)-1,1-dimethylurea and the second peak by ned-19 and antimycin A, indicating that NO synthesis is dependent on calcium release and occurs in organelles. The level of H_2O_2 increased at 2, 3, and 12 h and was inhibited by ned-19, ryanodine, xestospongin C, and moniliformin, indicating that H_2O_2 accumulation is dependent on calcium release and Krebs cycle activity. In addition, pyruvate dehydrogenase, 2-oxoxglutarate dehydrogenase, and isocitrate dehydrogenase activities of the Krebs cycle increased at 2, 3, 12, and/or 14 h, and these increases were inhibited in vitro by EGTA, a calcium chelating agent. Calcium release at 2, 3, and 12 h was inhibited by 2-(4-carboxyphenyl)-4,4,5,5-tetramethylimidazoline-1-oxyl-3-oxide and ascorbate, indicating activation by NO and H_2O_2. In addition, the level of antioxidant protein gene transcripts decreased with *N*-(6-aminohexyl)-5-chloro-1-naphtalene sulfonamide and staurosporine. Thus, there is a copper-induced cross talk among calcium, H_2O_2, and NO and a calcium-dependent activation of gene expression involving calmodulins and calcium-dependent protein kinases.

The marine macroalga *Ulva compressa* Linnaeus (Chlorophyta), formerly *Enteromorpha compressa* (Hayden et al., 2003), is a cosmopolitan heavy metal-tolerant species that dominates copper-enriched coastal areas in northern Chile (Ratkevicius et al., 2003) and other parts of the world (Villares et al., 2001; Pereira et al., 2009). *U. compressa* from copper-enriched coastal environments accumulated the metal and showed an increase in activity of the antioxidant enzyme ascorbate (ASC) peroxidase (AP), a decrease in the level of the antioxidant compound glutathione (GSH), and synthesis of ASC that was accumulated as dehydroascorbate (Ratkevicius et al., 2003). In addition, *U. compressa* cultivated in vitro with a sublethal concentration of copper (10 μM) showed a sustained increase in activities of the antioxidant enzymes AP and GSH reductase (GR) and in activity of the defense enzyme phenyl-ala ammonia lyase (González et al., 2010b).

On the other hand, *U. compressa* cultivated with 10 μM copper for 7 d showed increases of intracellular calcium at 2, 3, and 12 h and increases in hydrogen peroxide (H_2O_2) level at 3 and 12 h as well as a retarded wave of superoxide anions beginning at d 3 and increasing until d 7 (González et al., 2010b). In addition, it was shown that copper-induced intracellular calcium release originated exclusively in the endoplasmic reticulum (ER) and involved the activation of ryanodine-sensitive and inositol 1,4,5 triphosphate (IP_3)-sensitive calcium channels (González et al., 2010a), and production of H_2O_2 occurred exclusively in organelles (González et al., 2010b).

[1] This work was supported by Fondo Nacional de Desarrollo Científico y Tecnológico (Fondecyt) 1085041 to A.M.

* Corresponding author; e-mail alejandra.moenne@usach.cl.

The author responsible for distribution of materials integral to the findings presented in this article in accordance with the policy described in the Instructions for Authors (www.plantphysiol.org) is: Alejandra Moenne (alejandra.moenne@usach.cl).

[C] Some figures in this article are displayed in color online but in black and white in the print edition.

[W] The online version of this article contains Web-only data.

[OA] Open Access articles can be viewed online without a subscription.

www.plantphysiol.org/cgi/doi/10.1104/pp.111.191759

Thus, the existence of temporally coincident increases in calcium and H_2O_2 levels suggests the occurrence of a cross talk between these intracellular signals in response to copper excess.

Regarding the mechanisms governing cross talk between calcium and H_2O_2, it is known that micromolar concentrations of calcium directly activate mitochondrial NADH-synthesizing enzymes of the Krebs cycle, mainly isocitrate dehydrogenase (IDH) and 2-oxoxglutarate dehydrogenase (OGDH) in human and mammalian cells (Rutter and Denton, 1989; Rutter et al., 1989; Denton, 2009). In contrast, pyruvate dehydrogenase (PDH) is activated by a calcium-dependent phosphatase and, thus, is indirectly activated by calcium (Budde et al., 1988; Denton, 2009). In plants, PDH, IDH, and OGDH activities are indirectly regulated by calcium, and their activation is dependent on calmodulins (CaMs; McCormack and Denton, 1981; Miernyk et al., 1987; Budde et al., 1988). In addition, it was shown that calcium-dependent activation of Krebs cycle enzymes leads to an increase in NADH concentration enhancing mitochondrial electron transport and, thus, production of superoxide anions and H_2O_2 in human cells (Brookes et al., 2004; Camello-Almaraz et al., 2006; Hidalgo and Donoso, 2008). Moreover, it has been determined that H_2O_2 activates calcium release by oxidation of cysteines present in ryanodine- and IP_3-sensitive channels in human cells (Hidalgo, 2005; Hidalgo and Donoso, 2008), and nitric oxide (NO) synthesis activates calcium release by nitrosylation of thiol groups present in calcium channels (Eu et al., 1999; Pan et al., 2008). In plants, a cross talk between calcium and H_2O_2 has been described in Arabidopsis (*Arabidopsis thaliana*) guard cells exposed to abscisic acid (ABA) and fungal elicitors because H_2O_2 production stimulates calcium entry by activating calcium channels located in the plasma membrane (Pei et al., 2000; Klüsener et al., 2002). In addition, it was shown that the fungal elicitor cryptogein and plant cell wall-derived oligogalacturonides increase the H_2O_2 level, which, in turn, activates calcium channels in the plasma membrane of *Nicotiana plumbaginifolia* cells (Lecourieux et al., 2002). Moreover, the elicitor cryptogein activates NADPH oxidase in the plasma membrane of tobacco cells, leading to the consumption of NADPH, which, in turn, activates the pentose phosphate pathway that produced NADPH and induces the accumulation of glycolysis intermediates (Pugin et al., 1997).

On the other hand, heavy metals and metalloids such as copper, zinc, cadmium, aluminum, and arsenic induced NO synthesis in plants that is dependent on an NO synthase-like activity (Tewari et al., 2008; Ramos et al., 2009; Singh et al., 2009; Xiong et al., 2010; Xu et al., 2010). In addition, it was demonstrated that NO synthase is activated by calcium via CaMs in Arabidopsis (Ma et al., 2008). Moreover, the increase in NO level activates expression of antioxidant enzymes such as superoxide dismutase (SOD), AP, and GR (Ramos et al., 2009; Singh et al., 2009; Wang et al., 2010) and the defense enzyme phenyl-ala ammonia lyase (Wang et al., 2006). Furthermore, it has been shown that there is a cross talk between NO and calcium because NO activates calcium release in *N. plumbaginifolia* and grapevine (*Vitis vinifera*; Lamotte et al., 2006; Vandelle et al., 2006). In addition, there is a cross talk among calcium, reactive oxygen species, and NO induced by cadmium in pea (*Pisum sativum*) plants, but the mechanism linking calcium release with NO and H_2O_2 levels was not determined (Rodríguez-Serrano et al., 2009). Thus, copper excess may also induce an increase in NO level in *U. compressa* as well as a cross talk between calcium and NO.

Regarding calcium release and regulation of gene expression, it is well known that oscillations in intracellular calcium are decoded by three types of calcium-binding proteins corresponding to CaMs, calcium-dependent protein kinases (CDPKs), and calcineurin B-like proteins that interact with calcineurin B-like protein-interacting protein kinases (Kudla et al., 2010). In this sense, it has been determined that CaMs are involved in the activation of antioxidant enzyme gene expression, i.e., SOD, AP, and GR in maize (*Zea mays*) plants exposed to ABA and H_2O_2 (Hu et al., 2007). Moreover, CDPKs participate in the phosphorylation and activation of transcription factors such as ABF1 involved in ABA responses and RSG involved in gibberellin responses and, thus, in the regulation of gene expression (Zhu et al., 2007; Ishida et al., 2008). Therefore, calcium oscillations occurring in *U. compressa* in response to copper excess may determine activation of antioxidant proteins gene expression via CaMs and/or CDPKs.

In this work, we analyzed the potential cross talk among calcium, NO, and H_2O_2 and the calcium-dependent activation of gene expression that may involve CaMs and/or CDPKs. To this end, the marine alga *U. compressa* was cultivated in control condition, exposed to 10 μM copper or treated with inhibitors of calcium channels, ned-19, ryanodine, and xestospongin C, with inhibitors of organellar electron transport chains, 3-(3,4-dichlorophenyl)-1,1-dimethylurea (DCMU) and antimycin A, with an inhibitor of NO synthase, *N*(*G*)-monomethyl L-ariginine (L-NMMA), with an inhibitor of PDH, moniliformin, with a scavenger of NO, 2-(4-carboxyphenyl)-4,4,5,5-tetramethylimidazoline-1-oxyl-3-oxide (cPTIO), and with a scavenger of H_2O_2, ASC, and exposed to 10 μM copper for 24 h. The levels of NO, H_2O_2, and intracellular calcium were determined as well as the activities of NO synthase and Krebs cycle enzymes PDH, IDH, and OGDH. In addition, the direct activation of the latter enzymes by calcium was analyzed using EGTA, a calcium chelating agent. Furthermore, the relative level of transcripts encoding the antioxidant enzymes AP, peroxiredoxin (PRX), thioredoxin (TRX), GSH-*S*-transferase (GST), and the heavy-metal chelating protein metallothionein (MET) was analyzed in *U. compressa* cultivated in control conditions, exposed to 10 μM copper, or treated with the inhibitors of CaMs, *N*-(6-aminohexyl)-5-chloro-1-naphtalene

sulfonamide (W-7), and CDPKs, staurosporine, and exposed to 10 μM copper for 3 or 5 d.

RESULTS

Copper-Induced NO Synthesis Is Dependent on NO Synthase Activity, Calcium Release, and Electron Transport in Organelles

U. compressa cultivated with 10 μM copper for 24 h showed increases in NO level at 2 and 12 h of copper exposure (Fig. 1A). In addition, cooccurring increases in NO synthase activity were detected at 2 and 12 h of copper treatment (Fig. 1B), and these increases were completely inhibited by 1 mM L-NMMA, an inhibitor of NO synthase (data not shown). On the other hand, the increase in NO level detected at 2 h was inhibited by L-NMMA in 100%; by ned-19, an inhibitor of NAADP-dependent calcium channels, in 95%; by DCMU, an inhibitor of chloroplast PSII, in 100%; and by ASC, an H_2O_2 scavenger, in 48% (Fig. 1C). In addition,

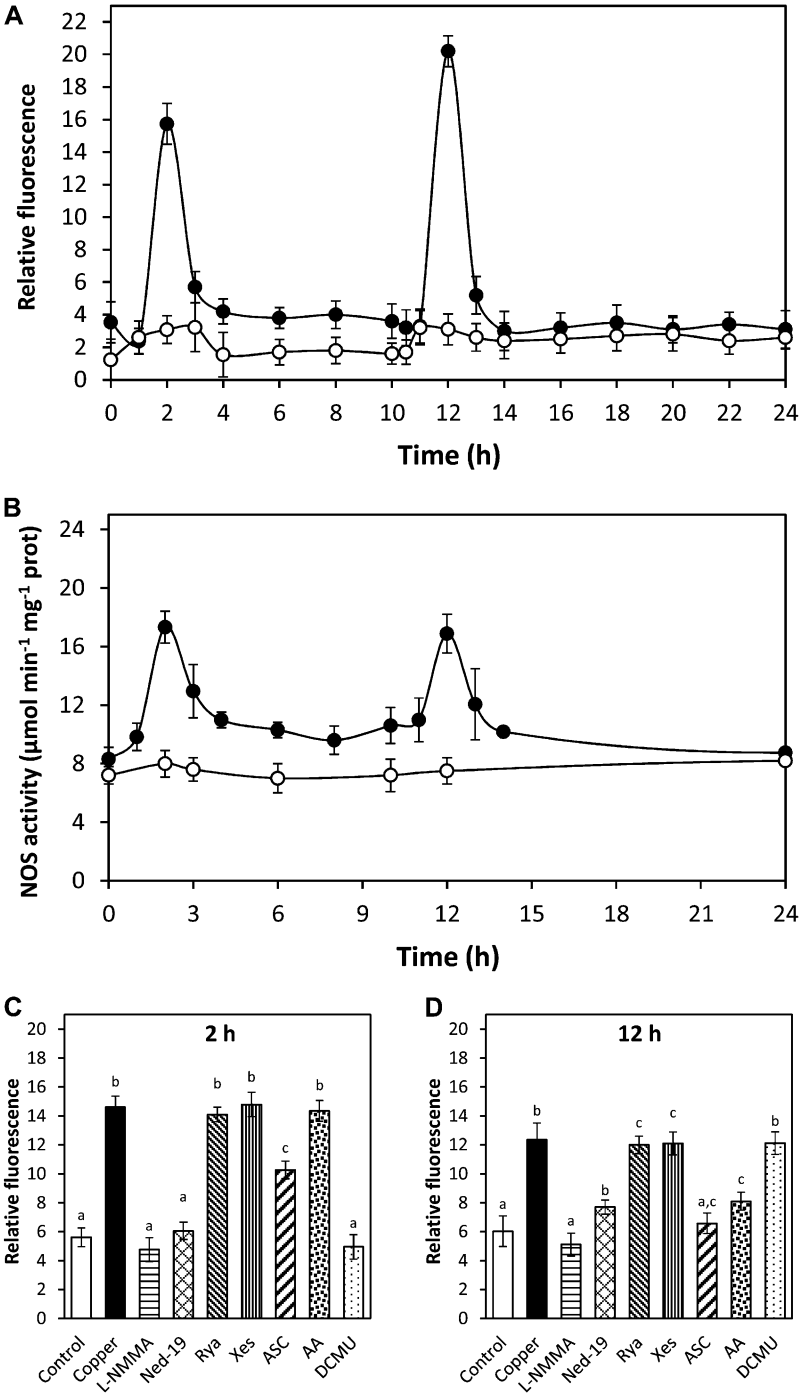

Figure 1. A, Level of NO in *U. compressa* cultivated in control condition (white circles) and exposed to 10 μM copper (black circles) for 24 h. NO level is expressed as the ratio between DAF-2 fluorescence and chloroplast autofluorescence. B, Activity of NO synthase in extracts of *U. compressa* cultivated in control condition (white circles) and exposed to 10 μM copper (black circles) for 24 h. NO synthase activity is expressed in micromoles per minute per milligram of protein. Level of NO in the alga cultivated in control condition (control), with 10 μM copper (copper) or treated with 1 mM L-NMMA, 10 μM ned-19, 100 μM ryanodine (rya), 10 μM xestospongin C (xes), 1 mM ASC, 10 μM AA, and 20 μM DCMU, and exposed to 10 μM copper for 2 h (C) and 12 h (D). Symbols and bars represent mean values of three independent replicates ± SD. Different letters indicate significant differences ($P < 0.05$).

the increase at 12 h was inhibited by L-NMMA in 100%; by ned-19 in 74%; by antimycin A (AA), an inhibitor of mitochondrial electron transport chain, in 67%; and by ASC in 93% (Fig. 1D). It is important to point out that the latter inhibitors did not change algal viability until 12 h of the experimental period (Supplemental Fig. S1). Thus, copper-induced NO synthesis is dependent on NO synthase activity, calcium release through NAADP-sensitive channels, electron transport in organelles, and H_2O_2 production, and occurs initially in chloroplasts and then in mitochondria.

Copper-Induced H_2O_2 Synthesis Is Dependent on Calcium Release, Electron Transport in Organelles, and Activation of the Krebs Cycle in Mitochondria

U. compressa cultivated with 10 μM copper for 24 h showed increases in H_2O_2 level at 2, 3, and 12 h of

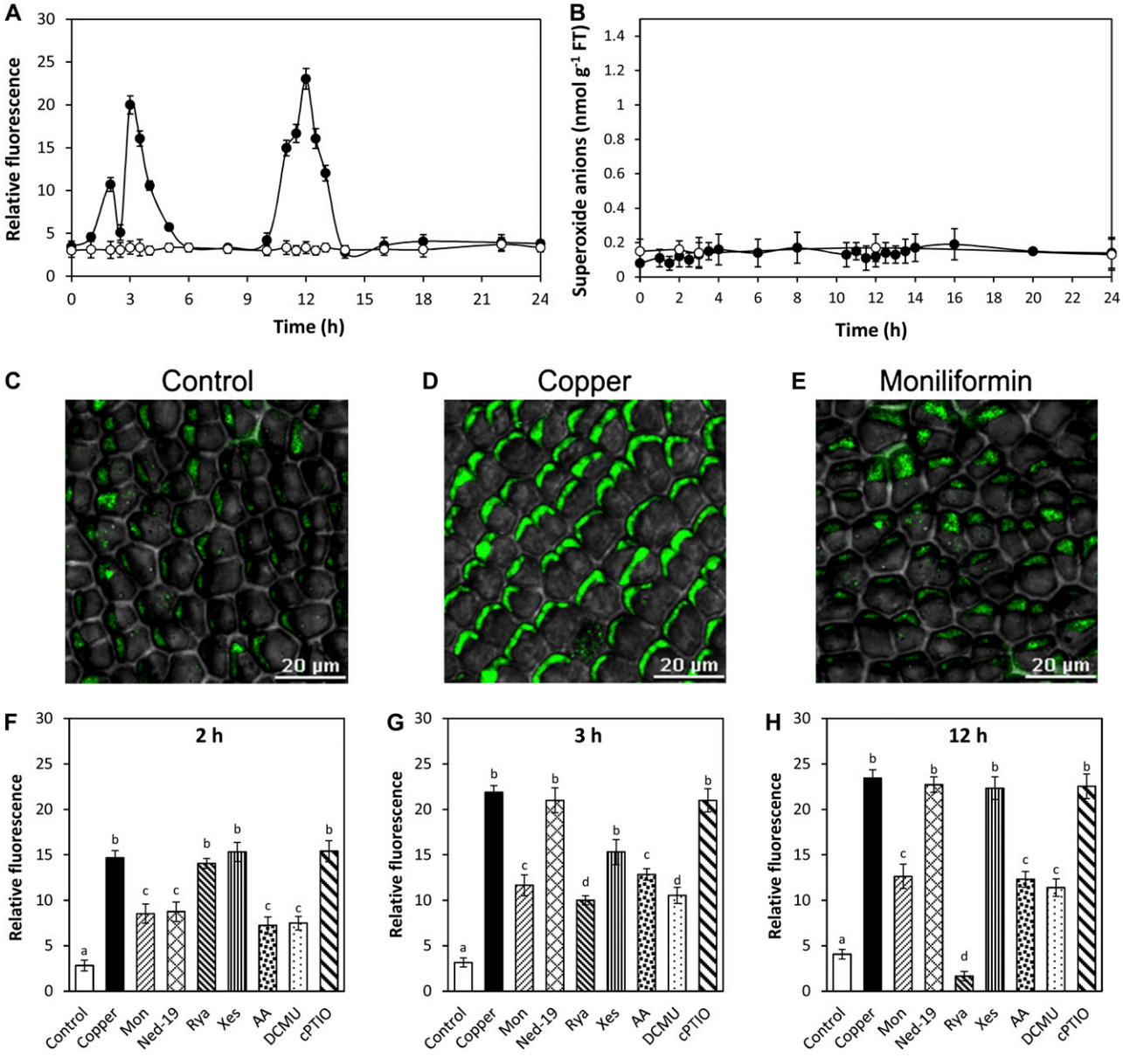

Figure 2. Level of H_2O_2 (A) and superoxide anions (B) in *U. compressa* cultivated in control condition (white circles) and exposed to 10 μM copper (black circles) for 24 h. Level of H_2O_2 is expressed as the ratio between dichlorofluorescein fluorescence and chloroplast autofluorescence. Visualization by confocal microscopy of H_2O_2 in *U. compressa* cultivated in control condition (C), exposed to 10 μM copper (D), or treated with 300 μM moniliformin and exposed to 10 μM copper (E) for 12 h. The white bar represents 20 μm. Level of H_2O_2 in the alga cultivated in control condition (control), exposed to 10 μM copper (copper), or treated with 300 μM moniliformin (mon), 10 μM ned-19, 100 μM ryanodine (rya), 10 μM xestospongin C (xes), 10 μM AA, 20 μM DCMU, and 1 mM cPTIO, and exposed to 10 μM copper for 2 h (F), 3 h (G), and 12 h (H). Symbols and bars represent mean values of three independent replicates ± SD. Different letters indicate significant differences ($P < 0.05$). [See online article for color version of this figure.]

copper exposure (Fig. 2A), whereas the level of superoxide anions remained at control level (Fig. 2B). In addition, increases in SOD activity were detected at 2 to 3 and 11 h of copper exposure (Supplemental Fig. S2), which explains the absence of superoxide anion accumulation. Moreover, the increases in H_2O_2 level at 2, 3, and 12 h were inhibited by moniliformin, an inhibitor of PDH activity, in 52%, 55%, and 56%, respectively, indicating that Krebs cycle activity is required for H_2O_2 production (Fig. 2, C–E). It is important to mention that PDH activity was inhibited in extracts of the alga cultivated with moniliformin and copper excess for 12 h (data not shown). Furthermore, the increase in H_2O_2 detected at 2 h was inhibited by ned-19 in 56%, by AA in 63%, and by DCMU in 61% and was not inhibited by cPTIO, an NO scavenger (Fig. 2E). The increase in H_2O_2 registered at 3 h was inhibited by ryanodine, an inhibitor of ryanodine-sensitive calcium channels, in 63%; by xestospongin C, an inhibitor of IP_3-dependent calcium channels, in 35%; by AA in 48%; and by DCMU in 61% and was not inhibited by cPTIO (Fig. 2F). The increase in H_2O_2 registered at 12 h was inhibited by ryanodine in 100%, in 62% by DCMU, and in 58% by AA and was not inhibited by cPTIO (Fig. 2G). Thus, copper-induced H_2O_2 synthesis is dependent on Krebs cycle activity, and calcium release by activation of different types of calcium channels occurs in chloroplast and mitochondria and is not dependent on NO synthesis.

On the other hand, activities of NADH-synthesizing enzymes of the Krebs cycle, PDH, IDH, and OGDH, showed increases at 2, 3, 12, and 14 h in *U. compressa* exposed to copper excess for 48 h (Fig. 3). In particular, PDH activity increased at 3, 12, and 14 h of copper exposure, decreased at 15 h, and remained at control level until 48 h (Fig. 3A). In addition, IDH activity increased at 2, 12, and 14 h of copper exposure but remained increased after 15 h (Fig. 3B). Moreover, OGDH activity increased at 2, 12, and 14 h of copper exposure and remained slightly increased after 15 h (Fig. 3C). Thus, transient increases in Krebs cycle enzyme activities are consistent with increases in H_2O_2 level observed at 2, 3, and 12 h, except for the increase at 14 h, which did not induce an increase in H_2O_2 level. In addition, increases in PDH activity at 3, 12, and 14 h were inhibited in vitro by EGTA, a calcium chelating agent, in 72%, 59%, and 100%, respectively (Fig. 4, A–C). Moreover, increases in IDH activity at 2, 12, and 14 h were inhibited by EGTA in 65%, 81%, and 61%, respectively (Fig. 4, D–F), and increases in OGH activity at 2, 12, and 14 h were inhibited in 85%, 70%, and 80%, respectively (Fig. 4, G–I). Thus, PDH, IDH, and OGDH enzymes of the Krebs cycle are directly activated by calcium.

Copper-Induced Calcium Release Is Dependent on the Activation of Three Types of Calcium Channels and Is Activated by NO and H_2O_2

U. compressa cultivated with 10 μM copper for 24 h showed increases in intracellular calcium at 2, 3, and 12 h, and these increases were inhibited by the calcium channel inhibitors ned-19, ryanodine, and xestospongin C (Fig. 5). In particular, calcium increase detected at 2 h was inhibited by ned-19, ryanodine, and xestospongin C in 89%, 84%, and 59%, respectively (Fig. 5A), the increase at 3 h was inhibited in 46%, 75%, and 82%, respectively (Fig. 5B), and the increase at 12 h was inhibited in 78%, 58%, and 36%, respectively (Fig. 5C). In addition, the calcium increase observed at 2 h was inhibited by ASC and cPTIO in 71% and 77%, respectively (Fig. 5A), the increase at 3 h was inhibited in 79% and 56%, respectively (Fig.

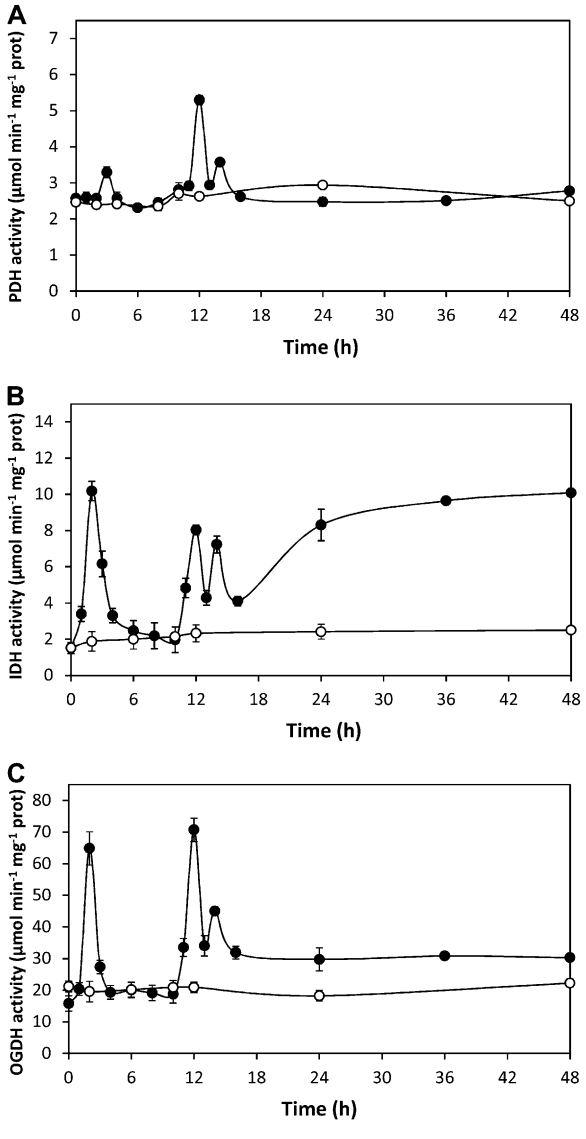

Figure 3. Activities of Krebs cycle enzymes PDH (A), IDH (B), and OGDH (C) in extracts of *U. compressa* cultivated in control condition (white circles) and exposed to 10 μM copper (black circles) for 48 h. Activities are expressed as micromoles per minute per milligram of protein. Symbols represent mean values of three independent experiments ± SD. Different letters indicate significant differences ($P < 0.05$).

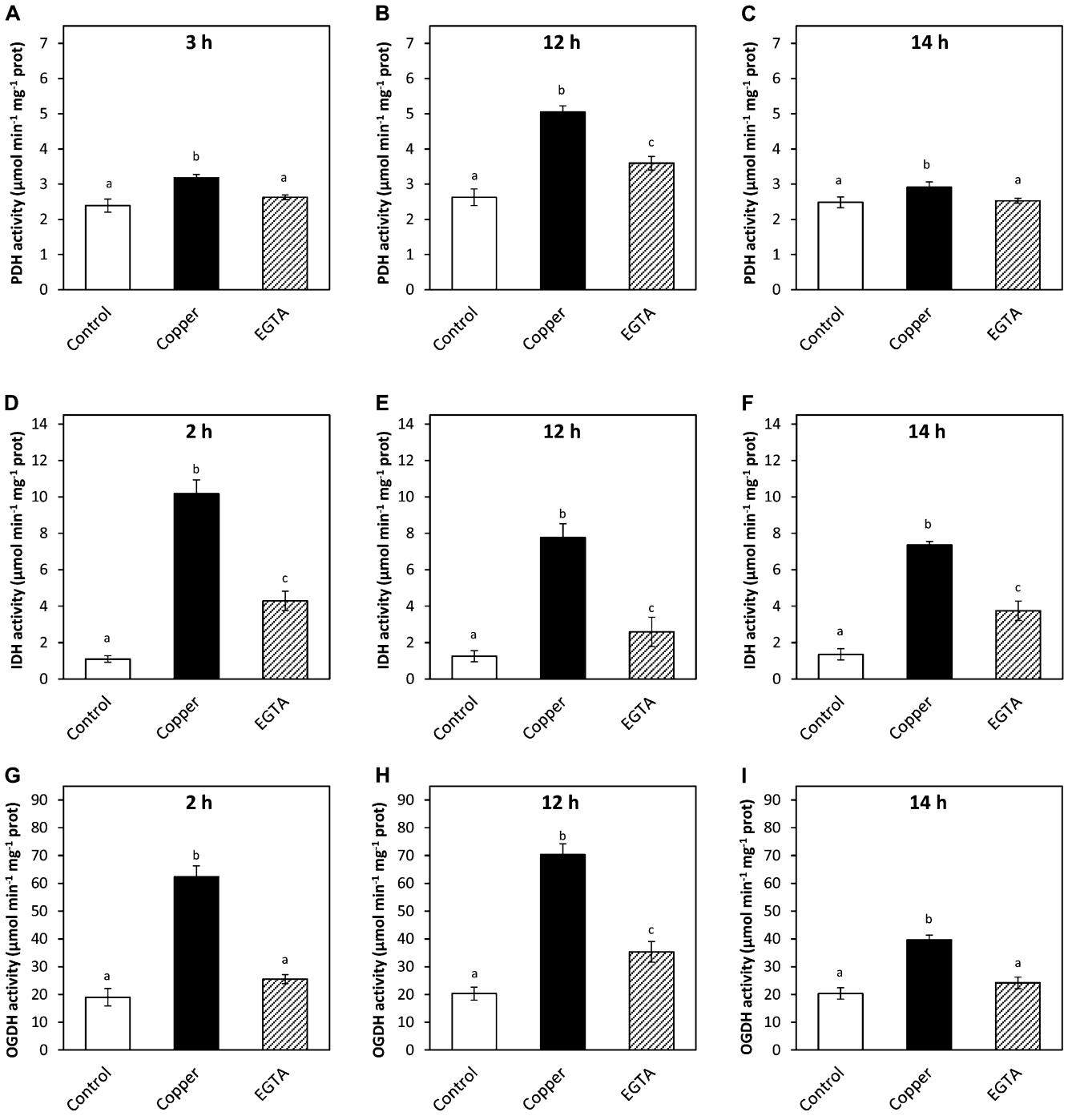

Figure 4. Activities of Krebs cycle enzymes PDH (A–C), IDH (D–F), and OGDH (G–I) in extracts of *U. compressa* cultivated in control condition (control) and exposed to 10 μM copper (copper) or in extracts of the alga cultivated with 10 μM copper for 2 h (D and G), 3 h (A), 12 h (B, E, and H), or 14 h (C, F, and I) and supplemented with 0.4 mM EGTA. Activities are expressed as micromoles per minute per milligram of protein. Bars represent mean values of three independent experiments ± SD. Different letters indicate significant differences ($P < 0.05$).

5C), and the increase at 12 h was inhibited in 81% and 62%, respectively (Fig. 5C). Thus, copper-induced calcium release involves the activation of NAADP-, ryanodine-, and IP_3-sensitive channels and is activated by NO and H_2O_2 synthesis.

Calcium Activates Antioxidant Protein Gene Expression via CaMs and CDPKs

U. compressa cultivated with 10 μM copper for 3 or 5 d showed increases in the level of transcripts encoding the antioxidant enzymes AP, PRX, TRX, and GST

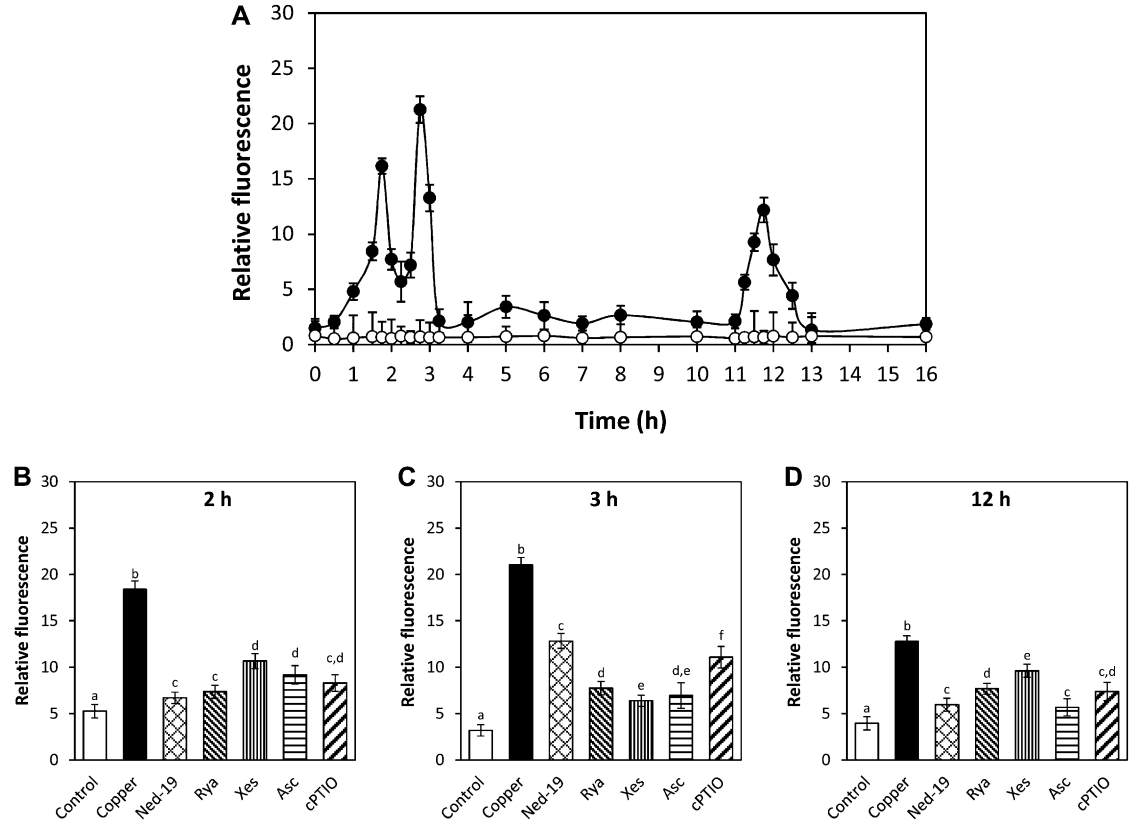

Figure 5. Level of intracellular calcium in *U. compressa* (A) cultivated in control condition (white circles) and with 10 μM copper (black circles). Calcium level is expressed as the ratio of Fluo 3 fluorescence and chloroplast autofluorescence. Level of calcium in the alga cultivated in control condition (control), exposed to 10 μM copper (copper), or treated with 10 μM ned-19, 100 μM ryanodine (rya), 10 μM xestospongin C (xes), 1 mM ASC, or 0.1 mM cPTIO and exposed to 10 μM copper for 2 h (B), 3 h (C), and 12 h (D). Bars represent mean values of three independent experiments ± SD. Different letters indicate significant differences ($P < 0.05$).

and in the heavy metal-chelating protein MET (Fig. 6). In addition, the relative level of transcripts coding for AP, PRX, TRX, GST, and MET decreased with W-7 in 44%, 86%, 75%, 14%, and 76%, respectively (Fig. 6, A–E), as well as with staurosporine in 61%, 80%, 77%, 84%, and 80%, respectively (Fig. 6, A–E). Thus, the copper-induced increase in intracellular calcium activates antioxidant proteins gene expression via CaMs and CDPKs.

DISCUSSION

Copper-Induced NO Synthesis Is Dependent on NO Synthase Activity, Calcium Release, and Electron Transport in Organelles

In this work, we showed that copper induced a biphasic increase in NO level that is dependent on NO synthase activity, calcium release, and electron transport in organelles. In this sense, it has been shown that copper and other heavy metals induced NO synthesis in plants and that its synthesis is dependent on an NO synthase-like activity (Tewari et al., 2008; Ramos et al., 2009; Singh et al., 2009; Xiong et al., 2010; Xu et al., 2010). In addition, it was determined that NO synthesis is dependent on calcium release in *N. plumbaginifolia* and grapevine (Lamotte et al., 2006; Vandelle et al., 2006). Moreover, a bacterial elicitor induces NO synthesis in Arabidopsis by an activation NO synthase activity via CaMs (Ma et al., 2008), and the bacterial elicitor flagellin activates calcium release and different CDPKs in Arabidopsis (Boudsocq et al., 2010). Thus, it is possible that copper-induced calcium-dependent activation of NO synthase in *U. compressa* may also involve CaMs and/or CDPKs.

Here, it was shown that copper-induced activation of NO requires release of intracellular calcium by activation of NAADP-sensitive channels. In this sense, it has been determined that NAADP-sensitive calcium channels are located in ER in terrestrial plants (Navazio et al., 2000), whereas they are found in lysosome-related acidic organelles in marine invertebrates and mammalian cells (Calcraft et al., 2009; Galione et al., 2010). In addition, we have previously shown that copper induced calcium release exclusively from ER in *U. compressa* (González et al., 2010a). Thus, NAADP-sensitive calcium channels in *U. compressa* might be located in ER as in terrestrial plants. Here, it was determined that copper-induced NO synthesis requires electron transport and occurs in organelles. In this sense, it has been shown that NO

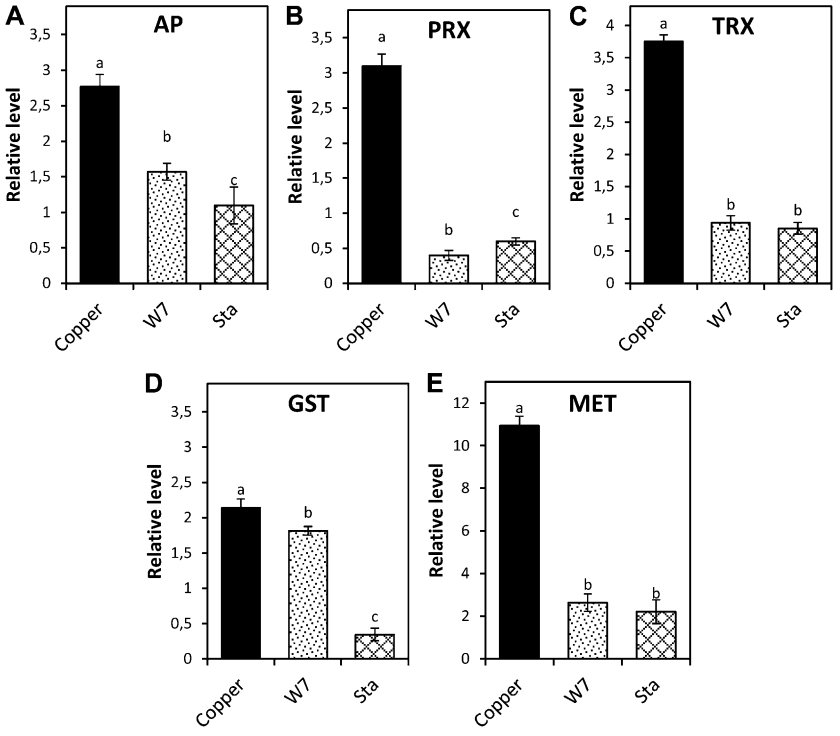

Figure 6. Relative level of transcripts encoding AP (A), PRX (B), TRX (C), GST (D), and MET (E) in *U. compressa* exposed to 10 μM copper (copper) and treated with 100 μM W-7 and 10 μM staurosporine (stau) for 3 d (AP, MET) or 5 d (PRX, TRX, GST). The relative level of transcripts is expressed as $2^{-\Delta\Delta CT}$. Bars represent mean values of three independent experiments ± SD. Different letters indicate significant differences ($P < 0.05$).

synthase activity is inhibited by DCMU, an inhibitor of PSII, in pea chloroplasts (Jasid et al., 2006) and that this enzyme is associated with mitochondrial complex I and is activated by electron transport in mammalian cells (Parihar et al., 2008). In addition, we determined that NO synthesis is activated by H_2O_2, which is produced by electron transport in organelles. Thus, it is possible that NO synthase activity requires electron transport in organelles because H_2O_2 activates calcium release (see below); in turn, calcium activates NO synthesis.

On the other hand, copper-induced NO synthesis occurs initially in chloroplast and then in mitochondria and involves calcium released from NAADP-sensitive calcium channels. In this sense, it has been shown that calcium can regulate photosynthesis and electron transport through CaMs that probably interact with PSII (Barr et al., 1982; Jarrett et al., 1982). In addition, it has been shown that mitochondria are in close contact with ryanodine-sensitive channels located in ER of human cells and that this proximity allows a rapid transfer of calcium from ER to the mitochondria (Csordás et al., 1999; Csordás and Hajnóczky, 2009). Thus, NAADP-sensitive channels located in ER of *U. compressa* may be in close contact with chloroplasts, which may favor the initial transfer of calcium from ER to chloroplast. Finally, there is an apparent inconsistency in our results because calcium release occurs at 2, 3, and 12 h and NO synthesis was only observed at 2 and 12 h. Based on present knowledge, it is difficult to explain such inconsistency, and additional research is required to clarify this point.

Copper-Induced H_2O_2 Synthesis Is Dependent on Calcium Release, Electron Transport in Organelles, and Activation of the Krebs Cycle in Mitochondria

Our results showed that copper induced increases in H_2O_2 level at 2, 3, and 12 h and that these increases required calcium release through different types of calcium channels as well as activation of the Krebs cycle and electron transport in organelles. In addition, we determined that NADH-synthesizing enzymes of the Krebs cycle, PDH, IDH, and OGDH, showed increases at 2, 3, and 12 h and that these enzymes are directly activated by calcium. Furthermore, we detected that SOD activity showed increases at 2 to 3 and 11 h of

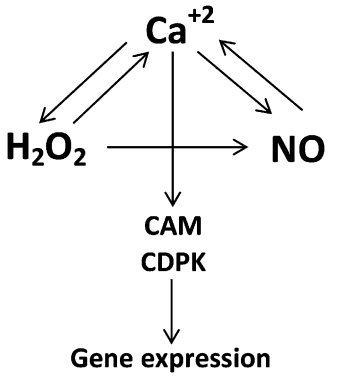

Figure 7. Schematic representation of the cross talk among calcium, NO, and H_2O_2 and the calcium-dependent activation of gene expression involving CaMs and CDPKs in *U. compressa* exposed to copper excess.

copper treatment. Thus, copper-induced calcium release activates mitochondrial NADH-synthesizing enzymes, leading to an increase in NADH, which may enter in mitochondrial complex I increasing electron transport and production of superoxide anions that are dismutated to H_2O_2 by SOD. In this sense, it is important to mention that NADH-synthesizing enzymes IDH and OGDH are directly activated by calcium in mammalian cells (Rutter and Denton, 1989; Rutter et al., 1989), whereas PDH activity is indirectly activated by calcium in mammalian cells and in plants (McCormack and Denton, 1981; Budde et al., 1988; Denton, 2009). Thus, the calcium-dependent regulation of PDH activity in *U. compressa* differs from what was observed in other eukaryotes, because this enzyme is directly activated by calcium. In addition, it is important to point out that calcium oscillations determine H_2O_2 and NO increases (see above), indicating that calcium orchestrates NO and H_2O_2 synthesis. However, NO and H_2O_2 are also required to activate calcium release (see below), indicating a mutual influence between these intracellular signals. However, there is an apparent inconsistency because activities of some Krebs cycle enzymes also increased at 14 h and H_2O_2 increases were observed only at 2, 3, and 12 h. The reason explaining the absence of an increase in H_2O_2 level at 14 h remained to be determined. Finally, it is important to point out that H_2O_2 activates NO synthesis, whereas the synthesis of NO is not required to activate H_2O_2 production (see a model in Fig. 7).

Copper-Induced Calcium Release Is Dependent on the Activation of Three Types of Calcium Channels and Is Activated by NO and H_2O_2

Here, we detected that copper-induced calcium release is dependent on NAADP-, ryanodine-, and IP_3-sensitive calcium channels. As mentioned before, it was previously determined that copper induced calcium release in *U. compressa* exclusively from ER, indicating that NAAD-, ryanodine-, and IP_3-sentive channels are located in the ER (González et al., 2010a). In addition, we showed that copper-induced calcium release is activated by NO and H_2O_2, indicating a cross talk between these intracellular signals. In this sense, it has been shown that ryanodine- and IP_3-sensitive calcium channels are regulated by H_2O_2 in human cells via oxidation of Cys residues (Hidalgo, 2005; Hidalgo and Donoso, 2008) and that NO regulates the activity of calcium channels via nitrosylation of thiol groups (Eu et al., 1999; Pan et al., 2008). Thus, NAADP-, ryanodine-, and IP_3-sensitive calcium channels in *U. compressa* are activated by H_2O_2 and NO, probably by oxidation and/or nitrosylation of thiol groups present in these calcium channels.

Calcium Activates Antioxidant Proteins Gene Expression via CaMs and CDPKs

Our results indicate that copper-induced calcium release activates antioxidant protein gene expression via CaMs and CDPKs. This is in accord with results obtained in maize plants treated with ABA and H_2O_2, where expression of antioxidant enzymes SOD, AP, and GR was activated by calcium via CaMs (Hu et al., 2007). It is important to mention that activation of antioxidant gene expression was also dependent on H_2O_2 and NO synthesis because it was inhibited by L-NMMA, an inhibitor of NO synthase, and diphenylene iodonium, an inhibitor of flavin-containing enzymes and organellar electron transport (data not shown), confirming the involvement of H_2O_2 and NO in activation of calcium release. In addition, it is not possible to exclude that H_2O_2 and NO may directly activate the expression of antioxidant protein genes via oxidation and/or nitrosylation of signal transduction proteins and/or transcription factors.

CONCLUSION

In this work, we showed that copper induced increases in calcium, NO, and H_2O_2 levels and that there is a cross talk between these intracellular signals, leading to a calcium-dependent activation of gene expression via calcium/CaMs and CDPKs in *U. compressa*.

MATERIALS AND METHODS

Algal and Seawater Sampling

Ulva compressa was collected in Cachagua (32° 34′S), a nonimpacted site of central Chile (Ratkevicius et al., 2003), during spring 2010 and transported to the laboratory in sealed plastic bags in a cooler at 4°C. Algal samples were rinsed three times in sterile filtered seawater and cleaned manually. Ultrasound was applied to remove epiphytic bacteria and organic debris twice for 1 min using a Branson 3200 ultrasound bath. Seawater was obtained from Quintay (33° 12′S) in central Chile, filtered through 0.45- and 0.2-μm pore size membrane filters, and stored in darkness at 4°C.

In Vitro Cultures

U. compressa was cultivated in filtered seawater without copper addition (control) or with 10 μM $CuCl_2$ (635 μg copper L^{-1}) at 12°C using a 12-h-light/12-h-dark photoperiod and a light intensity of 50 μmol m^{-2} s^{-1}. The culture medium was changed every 48 h. After sampling, material was treated with 100 mM Tris-HCl (pH 8.0) and 10 mM EDTA as the standard rinsing step prior to the different analyses.

Treatment with Inhibitors and Scavengers

The inhibitors of calcium channels used in this study were ned-19, chemically synthesized inhibitor of NAADP-dependent channels (Naylor et al., 2009); ryanodine, a plant alkaloid that inhibits ryanodine-sensitive calcium channels at a concentration of 100 μM (Meissner, 1986); xestospongin C, a marine sponge alkaloid that inhibits IP_3-sensitive calcium channels (Vassilev et al., 2001); L-NMMA, a competitive inhibitor of NO synthase activity (Olken et al., 1991); moniliformin, an inhibitor of PDH, which is the first enzyme of the Krebs cycle (Gathercole et al., 1986); AA, an inhibitor of mitochondrial complex III; DCMU, an inhibitor of PS II; cPTIO, an NO scavenger; ASC, an H_2O_2 scavenger; EGTA, a calcium chelating agent; W-7, a CaM inhibitor; and staurosporine, a CDPK inhibitor.

To analyze the inhibition of NO and H_2O_2 synthesis or that of intracellular calcium release in vivo, *U. compressa* (0.3 g of fresh tissue) was incubated in 1 mL of seawater containing 10 μM ned-19 (Enzo Life Sciences), 100 μM

ryanodine (Alexis Biochemicals), 10 μM xestospongin C (Sigma), 10 μM AA (Sigma), 20 μM DCMU (Sigma-Aldrich), or 300 μM moniliformin (Sigma) for 45 min or with 1 mM L-NMMA, 1 mM ASC, or 0.1 mM cPTIO for the entire experimental period. Algae were transferred to seawater without copper addition (0.15 g) or with 10 μM copper (0.15 g), cultivated for different experimental periods, and the levels of NO, H_2O_2, or calcium were analyzed by confocal microscopy. To analyze inhibition of Krebs cycle enzymes by EGTA in vitro, PDH, IDH, and OGDH activities were assayed in extracts supplemented with 0.4 mM EGTA. To analyze the inhibition of antioxidant protein gene expression, *U. compressa* (1 g) was incubated with 100 μM W-7 and 10 μM staurosporine for 1 h and cultivated with 10 μM copper for 3 or 5 d.

Detection of Cell Viability

Three lamina of *U. compressa* were incubated in 500 μL of filtered seawater containing 5 μM of Scyto-13 (Molecular Probes, Invitrogen) for 45 min, a fluorophore that stains nuclei of viable cells. A lamina of the alga was visualized by confocal microscopy using an Axiovert 100 confocal microscope (Carl Zeiss), emission wavelengths of 488 nm from an argon laser and 525 nm from a neon laser, and a filter of 505 to 530 nm for fluorescence detection.

Detection of NO, H_2O_2, and Calcium by Confocal Microscopy

Detection of calcium and H_2O_2 was performed as described by González et al. (2010b), and detection of NO was done as described by Lamotte et al. (2004). Three lamina of *U. compressa* were gently removed from culture media and incubated in seawater containing 20 μM 4,5 diaminofluorescein diacetate (DAF-2-DA) for NO detection, 10 μM of 2′,7′-dichlorohydrofluorescein diacetate (Calbiochem) for H_2O_2 detection, or 20 μM Fluo-3AM (Molecular Probes, Invitrogen) for calcium detection for 40 min at room temperature. The laminae were washed three times in filtered seawater to remove fluorophore excess. The green fluorescence of DAF-2, dichlorofluorescein, and Fluo 3 was visualized in each lamina by confocal microscopy using an Axiovert 100 confocal microscope (Carl Zeiss), an emission wavelength of 488 nm produced by an argon laser, and a filter of 505 to 530 nm. The intensity of green fluorescence and the red fluorescence of chloroplasts were quantified in each lamina using LSM510 software of the confocal microscope. The fluorescence intensity in each sample was normalized using chloroplast autofluorescence.

Detection of Superoxide Anions by Spectrofluorometry

U. compressa (5 g fresh weight) was cultivated in 150 mL of seawater without copper or with 10 μM copper for 0 to 24 h in triplicate. A sample of 1.5 g was incubated in 100 mL of Tris-HCl buffer (pH 7.0) containing 100 μM hydroethidine (Molecular Probes) for 45 min at room temperature. Algal tissue was rinsed in seawater, blotted dry, weighed, frozen in liquid nitrogen, and homogenized in a mortar with the addition of 5 mL of 40 mM Tris-HCl buffer (pH 7.5). The homogenate was centrifuged at 20,600*g* for 15 min, and the supernatant was recovered. Fluorescence of the clear extract was determined in an LS-5 spectrofluorometer (Perkin-Elmer) using an excitation wavelength of 480 nm and an emission wavelength of 590 nm. Superoxide anion level was expressed as nanomoles of 2-hydroxy ethidium using the extinction coefficient of 2-hydroxy ethidium (ξ = 9.4 mM^{-1} cm^{-1}).

Preparation of Protein Extracts

Protein extracts from *U. compressa* were prepared as described by Ratkevicius et al. (2003).

Detection of NO Synthase Activity

NO synthase activity was determined essentially as described by Ghigo et al. (2006). NO synthase activity was detected in 1 mL of reaction mixture containing 100 mM phosphate buffer (pH 7.0), 0.34 mM L-Arg, 2 mM magnesium chloride, 0.3 mM calcium chloride, 2 μM tetrahydrobiopterin, 1 μM FAD, 1 μM FMN, 0.2 mM dithiothreitol, 0.2 mM NADPH, and 80 μg of protein extract. The decrease in absorbance due to NADPH consumption was determined at 340 nm for 5 min. NOS activity was calculated using the extinction coefficient of NADPH (ε = 6.22 mM^{-1} cm^{-1}).

Detection of SOD Activity

SOD activity was determined as described by Beauchamp and Fridovich et al. (1971). SOD activity was detected in 1 mL of reaction mixture containing 30 mM Tris-HCl (pH 7.0), 0.1 mM EDTA, 20 μM riboflavin, 0.6 mM nitroblue tetrazolium (NBT), and 50 μg of protein extract. The reaction mixture and the control reaction without protein extract were incubated under white light for 15 min. The decrease in absorbance due to the inhibition of NBT reduction was detected at 560 nm. One unit of SOD activity was defined as the amount of enzyme that inhibits the photochemical reduction of NBT in 50% considering the absorbance of the control mixture as 100%.

Detection of Krebs Cycle Enzyme Activities

PDH activity was determined as described by Reid et al. (1977). PDH activity was detected in 1 mL of reaction mixture containing 100 mM Tris-HCl (pH 7.0), 20 mM magnesium chloride, 0.5 mM thiamine pyrophosphate, 1 mM lipoic acid, 0.13 mM CoA, 1 mM Cys, 2 mM sodium pyruvate, 1 mM NAD, and 5 μg of protein extract. The increase in absorbance due to NADH synthesis was detected at 340 nm for 1 min. PDH activity was calculated using the extinction coefficient of NADH (ε = 6.22 mM^{-1} cm^{-1}).

IDH activity was determined as described by Lemaitre et al. (2007). IDH activity was detected in 1 mL of reaction mixture containing 100 mM phosphate buffer (pH 7.0), 5 mM magnesium chloride, 10 mM sodium isocitrate, 1 mM NAD, and 40 μg of protein extract. The increase in absorbance due to NADH synthesis was detected at 340 nm for 3 min. IDH activity was calculated using the extinction coefficient of NADH (ε = 6.22 mM^{-1} cm^{-1}).

OGDH activity was determined as described by Millar et al. (1999). OGDH activity was detected in 1 mL of reaction mixture containing 150 mM Tris-HCl (pH 7.5), 20 mM magnesium chloride, 0.5 mM thiamine pyrophosphate, 1 mM lipoic acid, 0.13 mM CoA, 1 mM Cys, 2 mM sodium 2-oxoglutarate, 1 mM NAD, and 5 μg of protein extract. The increase in absorbance due to NADH synthesis was detected at 340 nm for 5 min. OGDH activity was calculated using the extinction coefficient of NADH (ε = 6.22 mM^{-1} cm^{-1}).

Quantification of Antioxidant Protein Transcript Levels

Total RNA (free of DNA) was extracted from 0.1 g of *U. compressa* using the FavorPrep Plant Total RNA kit (Favorgene) and quantified with the Quanti-iT Ribogreen RNA assay kit (Invitrogen). The relative level of transcripts coding for AP (accession no. FD387604), PRX (FD387607), TRX (FD387643), GST1 (FD387475), and MET (FD387450) and actin as internal control were amplified using a real-time thermocycler Rotor gene 6000 (Corbett Research). Real-time reverse transcription (RT)-PCR reactions were done using the Sensimix One-step kit (Quantace),11 ng of total RNA, 10 μM of each primer, and 3 mM magnesium chloride. PCR primers used to amplify AP transcripts were: forward-AP, 5′CCGACTATGCCACTTCAC 3′ and reverse-AP, 5′CTGCGATGCCACATTTCC3′; those to amplify PRX were forward-PRX, 5′CCAAGACGGTTGTGATGTTCGG3′ and reverse-PRX, 5′TGAGATTGAACGCACGCCATAC3′; those to amplify TRX were forward-TRX, 5′GAGCAGATGTCGGACGAGATTG3′and reverse-TRX, 5′TGAGATTGAACGCACGCCATAC3′; those to amplify GST were forward-GST, 5′CGACTTGTTGCGACGGTTTG3′ and reverse-GST, 5′TGCTCTTGAATGGACGACTGATG3′; those to amplify MET were forward-MET, 5′CTAGGTGAGGTGCCATTTTCG3′ and reverse-MET, 5′GTACGGTTACATACTTGGACAATG3′; and those to amplify actin were forward-ACT, 5′AGATTTGGCACCACACCTTC3′ and reverse-ACT, 5′CGATTCAACTTGGGGTTCAT3′. Real-time RT-PCR-amplified fragments were detected by fluorescence using SYBR GREEN I included in the amplification kit. Real-time RT-PCR reactions were performed using three independent replicates. Sample values were averaged, normalized using the $\Delta\Delta$CT method, and mean value control was subtracted from mean treated to determine fold of change in treated samples. The relative transcript level was expressed as $2^{-\Delta\Delta CT}$ (Livak and Schmittgen, 2001).

Statistical Analysis

Significant differences were determined by two-way ANOVA followed by Tukey's multiple comparison tests (*T*). Differences between mean values were considered to be significant at a probability of 5% ($P < 0.05$; Zar, 1999).

Supplemental Data

The following materials are available in the online version of this article.

Supplemental Figure S1. Visualization by confocal microscopy of cell viability in *U. compressa*.

Supplemental Figure S2. Activity of SOD in extracts of *U. compressa*.

Received November 30, 2011; accepted January 8, 2012; published January 10, 2012.

LITERATURE CITED

Barr R, Troxel KS, Crane FL (1982) Calmodulin antagonists inhibit electron transport in photosystem II of spinach chloroplasts. Biochem Biophys Res Commun **104:** 1182–1188

Beauchamp C, Fridovich I (1971) Superoxide dismutase: improved assays and an assay applicable to acrylamide gels. Anal Biochem **44:** 276–287

Boudsocq M, Willmann MR, McCormack M, Lee H, Shan L, He P, Bush J, Cheng SH, Sheen J (2010) Differential innate immune signalling via Ca (2+) sensor protein kinases. Nature **464:** 418–422

Brookes PS, Yoon Y, Robotham JL, Anders MW, Sheu SS (2004) Calcium, ATP, and ROS: a mitochondrial love-hate triangle. Am J Physiol Cell Physiol **287:** C817–C833

Budde RJ, Fang TK, Randall DD (1988) Regulation of the phosphorylation of mitochondrial pyruvate dehydrogenase complex *in situ*: effects of respiratory substrates and calcium. Plant Physiol **88:** 1031–1036

Calcraft PJ, Ruas M, Pan Z, Cheng X, Arredouani A, Hao X, Tang J, Rietdorf K, Teboul L, Chuang KT, et al (2009) NAADP mobilizes calcium from acidic organelles through two-pore channels. Nature **459:** 596–600

Camello-Almaraz C, Gómez-Pinilla PJ, Pozo MJ, Camello PJ (2006) Mitochondrial reactive oxygen species and Ca^{+2} signaling. Am J Physiol Cell Physiol **291:** C1082–C1088

Csordás G, Hajnóczky G (2009) SR/ER-mitochondrial local communication: calcium and ROS. Biochim Biophys Acta **1787:** 1352–1362

Csordás G, Thomas AP, Hajnóczky G (1999) Quasi-synaptic calcium signal transmission between endoplasmic reticulum and mitochondria. EMBO J **18:** 96–108

Denton RM (2009) Regulation of mitochondrial dehydrogenases by calcium ions. Biochim Biophys Acta **1787:** 1309–1316

Galione A, Morgan AJ, Arredouani A, Davis LC, Rietdorf K, Ruas M, Parrington J (2010) NAADP as an intracellular messenger regulating lysosomal calcium-release channels. Biochem Soc Trans **38:** 1424–1431

Gathercole PS, Thiel PG, Hofmeyr JH (1986) Inhibition of pyruvate dehydrogenase complex by moniliformin. Biochem J **233:** 719–723

Ghigo D, Riganti C, Gazzano E, Costamagna C, Bosia A (2006) Cycling of NADPH by glucose 6-phosphate dehydrogenase optimizes the spectrophotometric assay of nitric oxide synthase activity in cell lysates. Nitric Oxide **15:** 148–153

González A, Trebotich J, Vergara E, Medina C, Morales B, Moenne A (2010a) Copper-induced calcium release from ER involves the activation of ryanodine-sensitive and $IP(_3)$-sensitive channels in *Ulva compressa*. Plant Signal Behav **5:** 1647–1649

González A, Vera J, Castro J, Dennett G, Mellado M, Morales B, Correa JA, Moenne A (2010b) Co-occurring increases of calcium and organellar reactive oxygen species determine differential activation of antioxidant and defense enzymes in Ulva compressa (Chlorophyta) exposed to copper excess. Plant Cell Environ **33:** 1627–1640

Hayden HS, Blomster J, Maggs CA, Silva PC, Stanhope MJ, Waaland JR (2003) Linnaeus was right all along: *Ulva* and *Enteromorpha* are not distinct genera. Eur J Phycol **38:** 277–294

Hidalgo C (2005) Cross talk between Ca2+ and redox signalling cascades in muscle and neurons through the combined activation of ryanodine receptors/Ca2+ release channels. Philos Trans R Soc Lond B Biol Sci **360:** 2237–2246

Hidalgo C, Donoso P (2008) Crosstalk between calcium and redox signaling: from molecular mechanisms to health implications. Antioxid Redox Signal **10:** 1275–1312

Hu X, Jiang M, Zhang J, Zhang A, Lin F, Tan M (2007) Calcium-calmodulin is required for abscisic acid-induced antioxidant defense and functions both upstream and downstream of H2O2 production in leaves of maize (Zea mays) plants. New Phytol **173:** 27–38

Ishida S, Yuasa T, Nakata M, Takahashi Y (2008) A tobacco calcium-dependent protein kinase, CDPK1, regulates the transcription factor REPRESSION OF SHOOT GROWTH in response to gibberellins. Plant Cell **20:** 3273–3288

Jarrett HW, Brown CJ, Black CC, Cormier MJ (1982) Evidence that calmodulin is in the chloroplast of pea and serves as regulatory role in photosynthesis. J Biol Chem **257:** 13795–13804

Jasid S, Simontacchi M, Bartoli CG, Puntarulo S (2006) Chloroplasts as a nitric oxide cellular source. Effect of reactive nitrogen species on chloroplastic lipids and proteins. Plant Physiol **142:** 1246–1255

Klüsener B, Young JJ, Murata Y, Allen GJ, Mori IC, Hugouvieux V, Schroeder JI (2002) Convergence of calcium signaling pathways of pathogenic elicitors and abscisic acid in Arabidopsis guard cells. Plant Physiol **130:** 2152–2163

Kudla J, Batistic O, Hashimoto K (2010) Calcium signals: the lead currency of plant information processing. Plant Cell **22:** 541–563

Lamotte O, Courtois C, Dobrowolska G, Besson A, Pugin A, Wendehenne D (2006) Mechanisms of nitric-oxide-induced increase of free cytosolic Ca2+ concentration in Nicotiana plumbaginifolia cells. Free Radic Biol Med **40:** 1369–1376

Lamotte O, Gould K, Lecourieux D, Sequeira-Legrand A, Lebrun-Garcia A, Durner J, Pugin A, Wendehenne D (2004) Analysis of nitric oxide signaling functions in tobacco cells challenged by the elicitor cryptogein. Plant Physiol **135:** 516–529

Lecourieux D, Mazars C, Pauly N, Ranjeva R, Pugin A (2002) Analysis and effects of cytosolic free calcium increases in response to elicitors in Nicotiana plumbaginifolia cells. Plant Cell **14:** 2627–2641

Lemaitre T, Urbanczyk-Wochniak E, Flesch V, Bismuth E, Fernie AR, Hodges M (2007) NAD-dependent isocitrate dehydrogenase mutants of Arabidopsis suggest the enzyme is not limiting for nitrogen assimilation. Plant Physiol **144:** 1546–1558

Livak KJ, Schmittgen TD (2001) Analysis of relative gene expression data using real-time quantitative PCR and the $2^{(-\Delta\Delta C(T))}$ Method. Methods **25:** 402–408

Ma W, Smigel A, Tsai YC, Braam J, Berkowitz GA (2008) Innate immunity signaling: cytosolic Ca2+ elevation is linked to downstream nitric oxide generation through the action of calmodulin or a calmodulin-like protein. Plant Physiol **148:** 818–828

McCormack JG, Denton RM (1981) A comparative study of the regulation of Ca2+ of the activities of the 2-oxoglutarate dehydrogenase complex and NAD+-isocitrate dehydrogenase from a variety of sources. Biochem J **196:** 619–624

Meissner G (1986) Ryanodine activation and inhibition of the Ca2+ release channel of sarcoplasmic reticulum. J Biol Chem **261:** 6300–6306

Miernyk JA, Fang TK, Randall DD (1987) Calmodulin antagonists inhibit the mitochondrial pyruvate dehydrogenase complex. J Biol Chem **262:** 15338–15340

Millar AH, Hill SA, Leaver CJ (1999) Plant mitochondrial 2-oxoglutarate dehydrogenase complex: purification and characterization in potato. Biochem J **343:** 327–334

Navazio L, Bewell MA, Siddiqua A, Dickinson GD, Galione A, Sanders D (2000) Calcium release from the endoplasmic reticulum of higher plants elicited by the NADP metabolite nicotinic acid adenine dinucleotide phosphate. Proc Natl Acad Sci USA **97:** 8693–8698

Naylor E, Arredouani A, Vasudevan SR, Lewis AM, Parkesh R, Mizote A, Rosen D, Thomas JM, Izumi M, Ganesan A, et al (2009) Identification of a chemical probe for NAADP by virtual screening. Nat Chem Biol **5:** 220–226

Olken NM, Rusche KM, Richards MK, Marletta MA (1991) Inactivation of macrophage nitric oxide synthase activity by NG-methyl-L-arginine. Biochem Biophys Res Commun **177:** 828–833

Pan L, Zhang X, Song K, Wu X, Xu J (2008) Exogenous nitric oxide-induced release of calcium from intracellular IP3 receptor-sensitive stores via S-nitrosylation in respiratory burst-dependent neutrophils. Biochem Biophys Res Commun **377:** 1320–1325

Parihar MS, Nazarewicz RR, Kincaid E, Bringold U, Ghafourifar P (2008) Association of mitochondrial nitric oxide synthase activity with respiratory chain complex I. Biochem Biophys Res Commun **366:** 23–28

Pei ZM, Murata Y, Benning G, Thomine S, Klüsener B, Allen GJ, Grill E, Schroeder JI (2000) Calcium channels activated by hydrogen peroxide mediate abscisic acid signalling in guard cells. Nature **406:** 731–734

Pereira P, de Pablo H, Rosa-Santos F, Pacheco M, Vale C (2009) Metal accumulation and oxidative stress in Ulva sp. substantiated by response integration into a general stress index. Aquat Toxicol **91:** 336–345

Pugin A, Franchisse JM, Tavernier E, Bligny R, Gout E, Douce R, Guern J

(1997) Early events induced by the elicitor cryptogein in tobacco cells: involvement of a plasma membrane NADPH oxidase and activation of glycolisis and the pentose phosphate pathway. Plant Cell **9:** 2077–2091

Ramos J, Matamoros MA, Naya L, James EK, Rouhier N, Sato S, Tabata S, Becana M (2009) The glutathione peroxidase gene family of *Lotus japonicus*: characterization of genomic clones, expression analyses and immunolocalization in legumes. New Phytol **181:** 103–114

Ratkevicius N, Correa JA, Moenne A (2003) Copper accumulation, synthesis of ascorbate and activation of ascorbate peroxidase in *Enteromorpha compressa* (L.) Grev (Chlorophyta) from heavy metal-enriched environments in northern Chile. Plant Cell Environ **26:** 1599–1608

Reid EE, Thompson P, Lyttle CR, Dennis DT (1977) Pyruvate dehydrogenase complex from higher plant mitochondria and proplastids. Plant Physiol **59:** 842–848

Rodríguez-Serrano M, Romero-Puertas MC, Pazmiño DM, Testillano PS, Risueño MC, Del Río LA, Sandalio LM (2009) Cellular response of pea plants to cadmium toxicity: cross talk between reactive oxygen species, nitric oxide, and calcium. Plant Physiol **150:** 229–243

Rutter GA, Denton RM (1989) The binding of Ca2+ ions to pig heart NAD+-isocitrate dehydrogenase and the 2-oxoglutarate dehydrogenase complex. Biochem J **263:** 453–462

Rutter GA, Midgley PJ, Denton RM (1989) Regulation of the pyruvate dehydrogenase complex by Ca2+ within toluene-permeabilized heart mitochondria. Biochim Biophys Acta **1014:** 263–270

Singh HP, Kaur S, Batish DR, Sharma VP, Sharma N, Kohli RK (2009) Nitric oxide alleviates arsenic toxicity by reducing oxidative damage in the roots of *Oryza sativa* (rice). Nitric Oxide **20:** 289–297

Tewari RK, Hahn EJ, Paek KY (2008) Modulation of copper toxicity-induced oxidative damage by nitric oxide supply in the adventitious roots of Panax ginseng. Plant Cell Rep **27:** 171–181

Vandelle E, Poinssot B, Wendehenne D, Bentéjac M, Alain P (2006) Integrated signaling network involving calcium, nitric oxide, and active oxygen species but not mitogen-activated protein kinases in BcPG1-elicited grapevine defenses. Mol Plant Microbe Interact **19:** 429–440

Vassilev PM, Peng JB, Johnson J, Hediger MA, Brown EM (2001) Inhibition of CaT1 channel activity by a noncompetitive IP3 antagonist. Biochem Biophys Res Commun **280:** 145–150

Villares R, Puentes X, Carballeira A (2001) *Ulva* and *Enteromorpha* as indicators of heavy metal pollution. Hydrobiologia **462:** 221–232

Wang JW, Zheng LP, Wu JY, Tan RX (2006) Involvement of nitric oxide in oxidative burst, phenylalanine ammonia-lyase activation and Taxol production induced by low-energy ultrasound in Taxus yunnanensis cell suspension cultures. Nitric Oxide **15:** 351–358

Wang L, Yang L, Yang F, Li X, Song Y, Wang X, Hu X (2010) Involvements of H2O2 and metallothionein in NO-mediated tomato tolerance to copper toxicity. J Plant Physiol **167:** 1298–1306

Xiong J, Fu G, Tao L, Zhu C (2010) Roles of nitric oxide in alleviating heavy metal toxicity in plants. Arch Biochem Biophys **497:** 13–20

Xu J, Yin H, Li Y, Liu X (2010) Nitric oxide is associated with long-term zinc tolerance in *Solanum nigrum*. Plant Physiol **154:** 1319–1334

Xu L, Eu JP, Meissner G, Stamler JS (1998) Activation of the cardiac calcium release channel (ryanodine receptor) by poly-S-nitrosylation. Science **279:** 234–237

Zar J (1999) Biostatistical Analysis, Ed 4. Prentice Hall Inc., Englewood Cliffs, UK

Zhu SY, Yu XC, Wang XJ, Zhao R, Li Y, Fan RC, Shang Y, Du SY, Wang XF, Wu FQ, et al (2007) Two calcium-dependent protein kinases, CPK4 and CPK11, regulate abscisic acid signal transduction in *Arabidopsis*. Plant Cell **19:** 3019–3036